Two modes of polyamine block regulating the cardiac inward rectifier K^+ current I_{K1} as revealed by a study of the Kir2.1 channel expressed in a human cell line

Keiko Ishihara and Tsuguhisa Ehara

Department of Physiology, Saga Medical School, Saga 849-8501, Japan

The strong inward rectifier K^+ current, I_{K1}, shows significant outward current amplitude in the voltage range near the reversal potential and thereby causes rapid repolarization at the final phase of cardiac action potentials. However, the mechanism that generates the outward I_{K1} is not well understood. We recorded currents from the inside-out patches of HEK 293T cells that express the strong inward rectifier K^+ channel Kir2.1 and studied the blockage of the currents caused by cytoplasmic polyamines, namely, spermine and spermidine. The outward current–voltage (I–V) relationships of Kir2.1, obtained with 5–10 μM spermine or 10–100 μM spermidine, were similar to the steady-state outward I–V relationship of I_{K1}, showing a peak at a level that is ~20 mV more positive than the reversal potential, with a negative slope at more positive voltages. The relationships exhibited a plateau or a double-hump shape with 1 μM spermine/spermidine or 0.1 μM spermine, respectively. In the chord conductance–voltage relationships, there were extra conductances in the positive voltage range, which could not be described by the Boltzmann relations fitting the major part of the relationships. The extra conductances, which generated most of the outward currents in the presence of 5–10 μM spermine or 10–100 μM spermidine, were quantitatively explained by a model that considered two populations of Kir2.1 channels, which were blocked by polyamines in either a high-affinity mode (Mode 1 channel) or a low-affinity mode (Mode 2 channel). Analysis of the inward tail currents following test pulses indicated that the relief from the spermine block of Kir2.1 consisted of an exponential component and a virtually instantaneous component. The fractions of the two components nearly agreed with the fractions of the blockages in Mode 1 and Mode 2 calculated by the model. The estimated proportion of Mode 1 channels to total channels was 0.9 with 0.1–10 μM spermine, 0.75 with 1–100 μM spermidine, and between 0.75 and 0.9 when spermine and spermidine coexisted. An interaction of spermine/spermidine with the channel at an intracellular site appeared to modify the equilibrium of the two conformational channel states that allow different modes of blockage. Our results suggest that the outward I_{K1} is primarily generated by channels with lower affinities for polyamines. Polyamines may regulate the amplitude of the outward I_{K1}, not only by blocking the channels but also by modifying the proportion of channels that show different sensitivities to the polyamine block.

(Received 19 September 2003; accepted after revision 6 January 2004; first published online 14 January 2004)
Corresponding author K. Ishihara: Department of Physiology, Saga Medical School, 5-1-1 Nabeshima, Saga 849-8501, Japan. Email: keiko@post.saga-med.ac.jp

The outward current of the strong inward rectifier K^+ current, I_{K1}, plays an important role in the cardiac action potential. The outward I_{K1} is minimal at depolarized voltage levels, which is essential for generating long-lasting action potentials. On the other hand, the amplitude of the outward I_{K1} is large within the voltage range near the reversal potential (V_{rev}), and this outward I_{K1} produces rapid repolarization during the final phase of the cardiac action potentials (Luo & Rudy, 1994; Matsuoka *et al.* 2003). It is thus important to understand the mechanisms that determine the amplitude of the outward I_{K1}.

Recent progress in understanding the mechanism of the inward rectification (i.e. the property of the channel to open when the direction of the K^+ flux is inward and close when the direction of the K^+ flux is outward) of I_{K1} has been achieved from extensive studies on the cloned

 DOI: 10.1113/jphysiol.2003.055434

strong inward rectifier K^+ channels in the Kir2 subfamily (for a review, see Lopatin & Nichols, 2001; Stanfield *et al.* 2002). It is generally accepted that strong rectification is the result of a voltage-dependent blockage of the channel by cytoplasmic spermine and spermidine, which are ubiquitous polyamines in animal cells (Ficker *et al.* 1994; Lopatin *et al.* 1994; Fakler *et al.* 1995). Currently, the blockage of the channel by cytoplasmic Mg^{2+} (Matsuda *et al.* 1987; Vandenberg, 1987) is considered to play a role in increasing the amplitude of the outward I_{K1} during repolarization by inducing an outward transient of I_{K1} (Ishihara & Ehara, 1998; Ishihara *et al.* 2002).

Despite the above information, the flow of the outward I_{K1} during cardiac action potentials has not been quantitatively accounted for by the blockage of the channel by the cytoplasmic blockers. This is chiefly because the mechanism that generates the sustained outward current of I_{K1} in the voltage range between V_{rev} and a voltage that is ~60 mV more positive than V_{rev} remains unclear. The inward currents of the strong inward rectifier K^+ currents show a time-dependent activation phase, following an instantaneous current jump upon hyperpolarization (Hagiwara *et al.* 1976; Leech & Stanfield, 1981). The parameter of the time-dependent (activation) gating of I_{K1}, which is determined by analysing the amplitude of the activation phase, shows full 'deactivation' at a voltage that is ~30 mV more positive than V_{rev}; thus, the flow of the outward I_{K1} is not accounted for by this gating (Ishihara *et al.* 1989; Oliva *et al.* 1990). The time-dependent gating of Kir2.1, which strikingly resembles that of I_{K1}, is caused by the blockage of the channel by cytoplasmic spermine (Ishihara *et al.* 1996). Thus, it has been suggested that intracellular blockers of I_{K1}, other than spermine, play an important role in generating the outward currents. We previously demonstrated that the blockage of I_{K1} by cytoplasmic Mg^{2+} and its relief are practically instantaneous (Ishihara *et al.* 1989). Since the Mg^{2+} block traps the I_{K1} channel in subconductance states (Matsuda, 1988), the contribution of the Mg^{2+} block to the outward I_{K1} has been considered (Matsuda, 1988; Ishihara *et al.* 1989; Oliva *et al.* 1990). However, the steady-state outward current–voltage (I–V) relationship of the strong inward rectifiers is not significantly affected by varying the cytoplasmic free Mg^{2+} concentration (Silver & DeCoursey, 1990). The steady-state outward I–V relationships of the whole-cell I_{K1} measured in the previous studies, with different concentrations of cytoplasmic Mg^{2+}, were all similar to each other, i.e. the relationships showed a peak current at a voltage that is ~20 mV more positive than V_{rev} and a negative slope at more positive voltages, whether the currents were measured using pipette solutions containing very low concentrations of Mg^{2+} (Matsuda & Noma, 1984; Tourneur *et al.* 1987; Giles & Imaizumi, 1988; Oliva *et al.* 1990), using those containing ~1 mM Mg^{2+} (Ishihara & Ehara, 1998), or using the perforated-patch method (Ishihara *et al.* 2002). Thus, these observations contradict the notion that the Mg^{2+} block contributes significantly to the mechanism generating the sustained outward I_{K1}. The time courses of the relief from the blockages of the Kir2 channels by spermidine and putrescine (the immediate precursor of spermine and spermidine) have been demonstrated to be much faster than the relief from the spermine block (Kir2.3, Lopatin *et al.* 1995; Kir2.1, Ishihara *et al.* 1996). Previously, we demonstrated that putrescine can induce an outward transient of Kir2.1, as can Mg^{2+} (Ishihara, 1997). However, the low putrescine content in animal cells (see, for example, He *et al.* 1993) (with the exception of stage V–VI *Xenopus* oocytes that contain a high level of putrescine, but only a background level of spermine; Shinga *et al.* 1996) implies that putrescine does not contribute significantly to the inward rectification of I_{K1}. Thus, spermidine was the possible candidate as the molecule that plays an important role in generating the outward I_{K1}.

The Kir2.1 channel (IRK1; Kubo *et al.* 1993) is considered to provide the major fraction of I_{K1} in cardiac ventricular cells (Nakamura *et al.* 1998; Zaritsky *et al.* 2001), and the properties of Kir2.1 channels, examined by the whole-cell recordings, are very similar to those of I_{K1} (Stanfield *et al.* 1994*a*; Ishihara *et al.* 1996). In this study, we expressed the Kir2.1 channel in HEK 293T cells and analysed the macroscopic currents recorded from excised inside-out patches in the presence of various concentrations of cytoplasmic polyamines. Contrary to our expectation, the outward I–V relationship and the time-dependent gating of the Kir2.1 channel, in the presence of ~5 μM spermine alone, are similar to those of I_{K1}. The analysis of the chord conductance–voltage (G–V) relationships in the present study strongly suggests that a small population of channels is less sensitive to the polyamine block than the other channels. Our results suggest that the steady-state outward I–V relationship of I_{K1} is chiefly determined by the spermine block of the channels that exhibit lower affinities to cytoplasmic polyamines.

Methods

Expression of *IRK1* gene in HEK 293T cells

The mouse *IRK1* gene (a gift from Professor L.Y. Jan, University of California, San Francisco, CA, USA),

previously subcloned into the mammalian expression vector pCXN2 (Ishihara *et al.* 1996), was used for the present study. HEK 293T cells (derived from the human embryonic kidney cell line 293 and containing the SV 40 large T antigen) were grown in Dulbecco's modified Eagle's medium (Gibco-BRL, Gaithersburg, MD, USA) supplemented with 10% heat-inactivated fetal bovine serum (Gibco-BRL), 0.15% sodium bicarbonate, penicillin (200 U ml^{-1}), and streptomycin (200 μg ml^{-1}). Cells were plated at 1.5×10^5 cells per 30 mm dish, 1 day prior to transfection. The cells were transfected with 0.4 μg of pCXN2-IRK1 and 0.04 μg of plasmid DNA encoding the green fluorescent protein (pEGFP-N1; Clontech, Palo Alto, CA, USA) using an Effectene transfection reagent (Qiagen Inc., CA, USA). Autofluorescence was visualized using an inverted fluorescence microscope to identify the cells expressing exogenous genes.

Solutions

The pipette (extracellular) solution contained (mM): 145 KCl, 1 $CaCl_2$ and 5 Hepes (pH 7.4 with ~2 mM KOH). The bath solution used as the control Mg^{2+}-free, polyamine-free cytoplasmic solution contained (mM): 125 KCl, 4 EDTA (2K), 7.2 K_2HPO_4 and 2.8 KH_2PO_4 (pH 7.2 with ~3 mM KOH). The free Mg^{2+} and Ca^{2+} concentrations in this solution were calculated to be at submicromolar levels (Fabiato & Fabiato, 1979), assuming that the amounts of Ca^{2+} and Mg^{2+} contained in the solution were ~10 μM each. The stock solutions, containing 10 mM of spermine/spermidine, were prepared by dissolving spermine-4Cl (Nacalai Tesque, Kyoto, Japan) or spermidine-3Cl (Nacalai Tesque) in distilled water and were stored in small aliquots at –20°C. Before the experiment the cytoplasmic solutions, containing various concentrations of spermine/spermidine, were prepared by diluting these stock solutions with the control Mg^{2+}-free, polyamine-free cytoplasmic solution to the desired concentrations.

Current recordings from HEK 293T cells expressing Kir2.1

On the day of transfection or on the day of recording the data, the cells were trypsinized using 0.25% trypsin–EDTA solution (Sigma) and seeded onto small pieces of collagen-coated coverglass (Asahi Techno Glass Corporation, Tokyo, Japan), such that they could be placed in the recording chamber (area: 5 mm × 20 mm; volume: ~0.5 ml), which was mounted on the stage of an inverted fluorescence microscope (TMD300; Nikon, Tokyo, Japan).

At 24–56 h after the transfection, currents were recorded from inside-out patch membranes by the conventional patch-clamp technique (Hamill *et al.* 1981) using a patch-clamp amplifier (Axopatch 200B, Axon Instruments, Union City, CA, USA). Before the experiment, pipettes made from hard borosilicate glass capillaries (1.5 mm o.d., 1.0 mm i.d.; Narishige, Tokyo, Japan) using a horizontal puller (Sutter Instruments, Novato, CA, USA) were coated with silicone (Shin-Etsu Chemical, Tokyo, Japan) and then heat-polished. The resistance of the electrodes filled with the pipette solution was 2–2.5 MΩ. The recording chamber was continuously perfused with a fresh bath solution at the rate of ~3 ml min^{-1}, and the excised patch membrane was located near the site where the bath solution flowed into the recording chamber. The effects of the cytoplasmic polyamines were examined after the native inward rectification had been removed to as great an extent as possible in the control Mg^{2+}-free, polyamine-free cytoplasmic solution. Voltage stimulations and data acquisitions were performed using pCLAMP8 software (Axon Instruments) on a Pentium PC through a 12 bit AD converter (Digidata 1200A, Axon Instruments). Currents were filtered at 5–10 kHz and sampled at 25–50 kHz. Capacitive currents were compensated for by using the patch-clamp amplifier. The holding potential was 0 mV. The horizontal dotted lines superimposed on the current traces indicate the zero-current level. To measure *I–V* relationships, test pulses were usually applied between −60 and +90 mV in 5 mV steps. A hyperpolarizing pre-pulse to −40 mV was used before applying a test pulse, to relieve most of the channels from blockage by cytoplasmic Kir2.1 blockers. All experiments were conducted at room temperature (24–26°C).

Analysis of Kir2.1 currents

To evaluate the blockage of Kir2.1 currents by polyamines, we used the chord conductance values calculated from the *I–V* relationships using the equation $G = I/(V-V_{rev})$. Current amplitudes were usually measured at ~200 ms after the onset of the step pulses. V_{rev} values were determined using a ramp pulse (0.4–4 V s^{-1}) and were always near 0 mV (0–2 mV), in agreement with the K^+ equilibrium potential of ~1 mV predicted from the experimental conditions. The small discrepancy could be partially attributed to the junction potential between the pipette and the cytoplasmic solutions, which was not corrected for in this study. For the results, conductance values were normalized with respect to the maximum value obtained using large negative pulses (G/G_{max}). In the cases where the application of relatively high concentrations of

polyamines reduced the amplitude of the inward currents in the entire negative voltage range measured (Fig. 2), the conductance values were normalized with the maximum conductance value that had been obtained in the absence of or with lower concentrations of polyamines.

Curve fittings and statistics

Least-squares fits were performed using the algorithms incorporated in Microcal Origin (ver. 6, Microcal Software, Northampton, MA, USA) and pCLAMP software. The statistical values are given as the means ± S.E.M. (*n*, number of experiments).

Results

Outward *I–V* relationships of Kir2.1 in the presence of cytoplasmic spermine and spermidine

We first tried to identify the spermine and spermidine concentrations at which the Kir2.1 channel exhibits outward *I–V* relationships similar to the steady-state outward *I–V* relationship of I_{K1}. Figure 1*A* shows Kir2.1 currents recorded from inside-out patch membranes by applying different amounts of spermine or spermidine to the cytoplasmic solution after the native inward rectification had been removed to as great an extent as possible in the control Mg^{2+}-free, polyamine-free cytoplasmic solution. In the presence of 0.1–10 μM

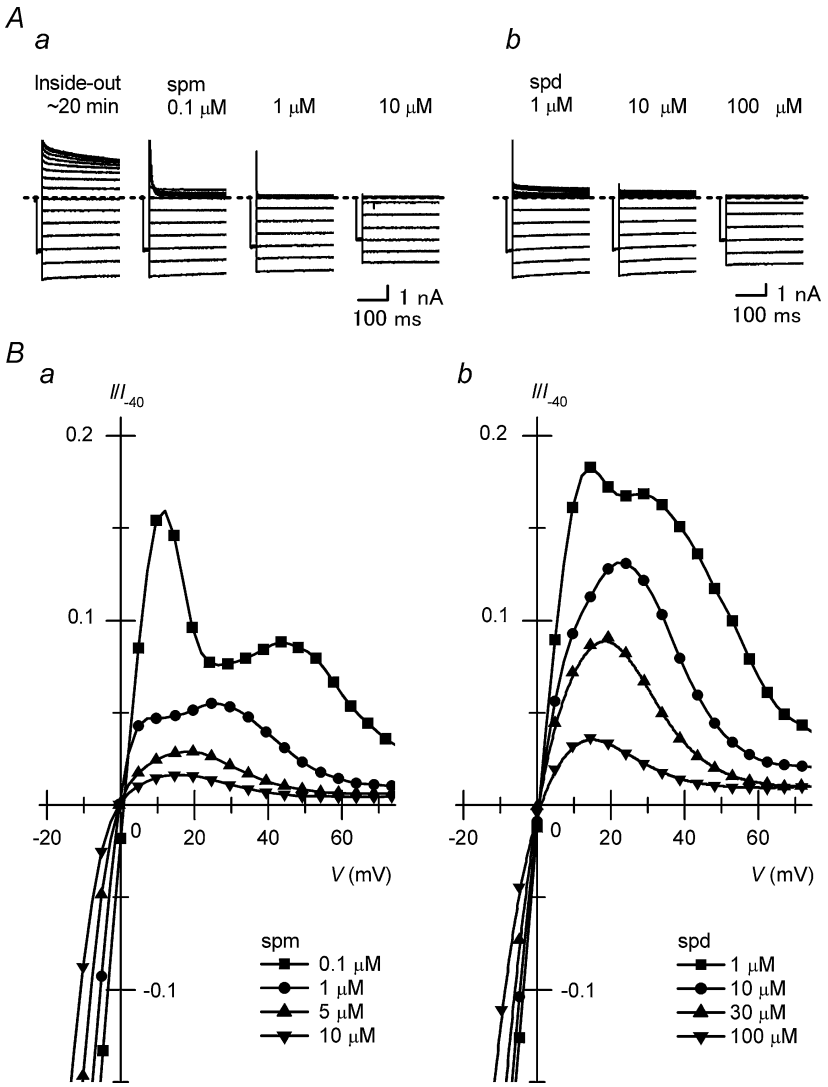

Figure 1. Outward *I–V* relationships of Kir2.1 currents in the presence of cytoplasmic spermine and spermidine
A, families of currents recorded from a patch membrane in the presence of 0.1, 1 and 10 μM spermine (spm; *a*) or 1, 10 and 100 μM spermidine (spd; *b*) using test pulses between –60 and +80 mV in 10 mV steps. Currents recorded in the control polyamine-free, Mg^{2+}-free cytoplasmic solution at ~20 min after the patch excision are also shown in (*a*). In this study, current recordings were made at room temperature and symmetrical $[K^+]$ of ~150 mM. Currents shown in *Aa* and *Ab* were obtained from different patches. *B*, *I–V* relationships in the presence of 0.1 μM (■), 1 μM (●), 5 μM (▲), 10 μM (▼) spermine (*a*); and 1 μM (■), 10 μM (●), 30 μM (▲), 100 μM (▼) spermidine (*b*). Currents shown in *A* were selected from those used to obtain these relationships. Current amplitudes are normalized with respect to the inward current amplitude at −40 mV measured with 0.1 μM spermine (*a*) or 1 μM spermidine (*b*).

spermine (Fig. 1*Aa*) or 1–100 μM spermidine (Fig. 1*Ab*), the outward currents were rapidly suppressed during the depolarizing steps. Figure 1*Ba* and *b* show the outward *I–V* relationships obtained with 0.1–10 μM spermine and 1–100 μM spermidine, respectively. The current amplitudes in these plots are normalized with respect to the inward current amplitude at −40 mV measured with 0.1 μM spermine or 1 μM spermidine that did not notably block the currents at −40 mV. The amplitudes of the outward currents observed with these concentrations of spermine were smaller than those obtained with approximately 10-fold concentrations of spermidine. The steady-state *I–V* relationship of the outward currents obtained with 0.1 μM spermine showed two distinct peaks (see also Guo & Lu, 2000*a*) and that with 1 μM spermine or spermidine showed a plateau. These *I–V* relationships were different in shape from the steady-state *I–V* relationship of I_{K1}. All the outward *I–V* relationships obtained with 5–10 μM spermine and with 10–100 μM spermidine showed a peak at a voltage near V_{rev} +20 mV and a negative slope at more positive voltages, similar to the steady-state outward *I–V* relationship of I_{K1} (e.g. Ishihara *et al.* 2002).

G–V relationships of Kir2.1 in the presence of cytoplasmic polyamines

To examine the voltage dependence of the polyamine block of the Kir2.1 channel, we analysed the *G–V* relationships of the Kir2.1 currents recorded in the presence of 0.1–10 μM spermine and 1–100 μM spermidine (Fig. 2). The *G–V* relationships shifted towards the left as the polyamine concentration increased, in agreement with the voltage-dependent blockage of the channel by these molecules. The half-blocking voltages ($V_{1/2}$) of spermine were +12.5 mV (0.1 μM), +1 mV (1 μM), −8 mV (5 μM), and −13 mV (10 μM), and those of spermidine were +16.5 mV (1 μM), +4.5 mV (10 μM), −3 mV (30 μM), and −14.5 mV (100 μM).

Further, two other features were noted in the *G–V* relationships. First, with relatively high concentrations of

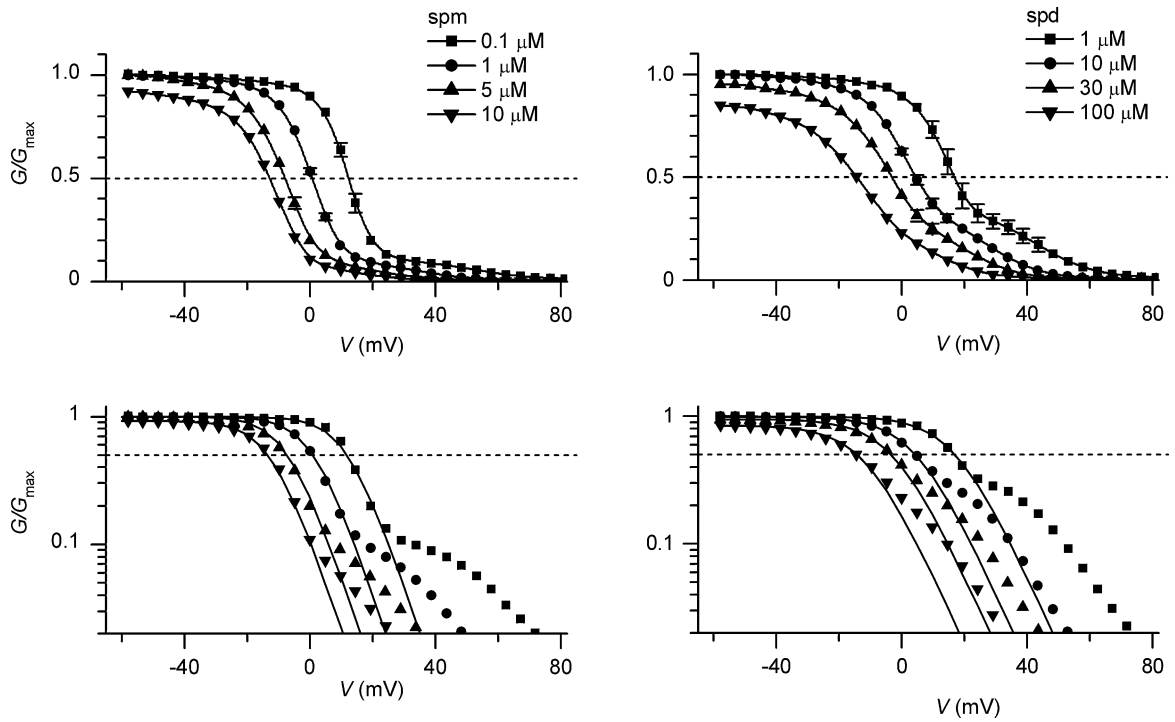

Figure 2. *G–V* relationships of Kir2.1 currents obtained with various concentrations of cytoplasmic polyamines

Left, spermine (spm) 0.1 μM (■), 1 μM (●), 5 μM (▲), 10 μM (▼). Right, spermidine (spd) 1 μM (■), 10 μM (●), 30 μM (▲), 100 μM (▼). Data are the means of 3–12 experiments. Error bars are not shown if they were smaller than the symbols. $G/G_{max} = 0.5$ is shown by a horizontal dotted line to indicate $V_{1/2}$. The same *G–V* relationships are plotted on a semilogarithmic scale in the lower panels. The continuous lines in the lower panels show the fits with Boltzmann relations to values at around $V_{1/2}$. The slope factor of the Boltzmann relations was ∼6 mV with spermine and ∼8 mV with spermidine.

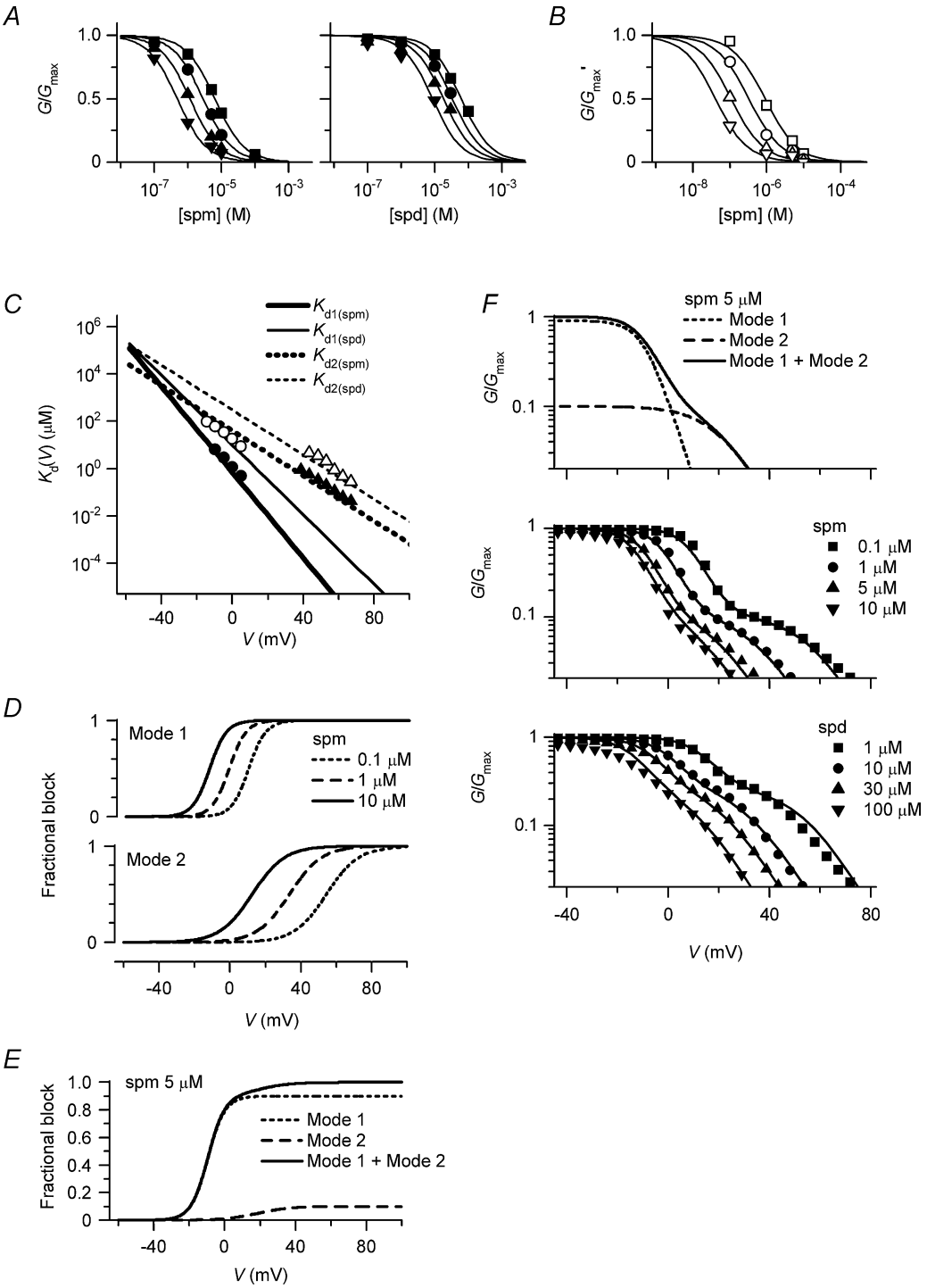

Figure 3. A model reconstructing *G–V* relationships of Kir2.1 obtained in the presence of polyamines
A, dose–response relationships of the spermine block (spm; left) and the spermidine block (spd; right) examined at −10 (■), −5 (●), 0 (▲) and +5 mV (▼). G/G_{max} values are the mean values of the data shown in Fig. 2. The Hill equation, $G/G_{max} = (1 + [PA]/K_d)^{-1}$, is fitted to each relationship. *B*, normalized dose–response relationships of the spermine block at +40 (□), +50 (○), +60 (△) and +70 mV (▽). The values of G/G_{max}' shown were obtained by normalizing the G/G_{max} values with the maximum value in the voltage range between +40 and +70 mV after subtracting a minute background conductance. Similar analyses were performed for the spermidine block. *C*, voltage dependences of the $K_d(V)$ values of the spermine block (thick lines) and the spermidine block (thin lines) in Mode 1 ($K_{d1(spm)}(V)$ and $K_{d1(spd)}(V)$; continuous lines) and Mode 2 ($K_{d2(spm)}(V)$ and $K_{d2(spd)}(V)$; dotted lines). The K_d values obtained from dose–response relationships are shown by symbols (filled symbols,

the polyamines (10 μM spermine, 30 μM spermidine, and 100 μM spermidine), conductances at the negative voltages (<-20 mV) became small and the relationships in this voltage range exhibited a weak voltage dependence. These findings resulted from the apparent shift of the inward *I–V* relationships to the negative side (data not shown; see Xie *et al.* 2002). G/G_{max} values at -60 mV were 0.92 ± 0.007 ($n = 7$), 0.95 ± 0.005 ($n = 4$), and 0.85 ± 0.01 ($n = 4$) with 10 μM spermine, 30 μM spermidine, and 100 μM spermidine, respectively.

Second, as the polyamine concentration decreased, conductances at voltages more positive than $V_{1/2} + \sim$10 mV increased, which was observed even more clearly by plotting the *G–V* relationships on a semilogarithmic scale (Fig. 2, lower panels). As shown by the continuous lines, the strong voltage dependence of the conductances observed around $V_{1/2}$ can be described by the Boltzmann relation:

$$G/G_{max} = 1/(1 + \exp((V - V_h)/s)) \quad (1)$$

where V_h and s indicate the half-activation voltage and the slope factor, respectively. At voltages more positive than $V_{1/2} + \sim$10 mV, there were 'extra conductances' that could not be described by the fitted Boltzmann relations. These extra conductances corresponded to the majority of the outward currents that flowed in the presence of 5–10 μM spermine/10–100 μM spermidine (Fig. 1*B*). In the case of the *G–V* relationships obtained with spermine, it appeared that the extra conductances could be fitted with the Boltzmann relation, in which the maximum level was $\sim$0.1, and the V_h value increasingly became more positive than the $V_{1/2}$ value as the concentration decreased (fits not shown, but see the top panel of Fig. 3*F*). This finding was essentially the same in the case of spermidine, although the maximum level of extra conductances seemed to be larger, i.e. 0.2–0.3. These observations led us to hypothesize that polyamines may block the Kir2.1 channel in two distinct modes, a high-affinity mode and a low-affinity mode. The steep voltage dependence of the *G–V* relationships (fitted with Boltzmann relations in lower panels of Fig. 2) may reflect the polyamine block of the major fraction of channels in the high-affinity mode. On the other hand, extra conductances may be generated by a fraction of channels that were blocked by polyamines in the low-affinity mode. The ratio of the channels accepting respective modes of blockage did not appear to be significantly affected by the concentration of polyamines, whereas the ratio was affected by the species of polyamine present in the cytoplasmic solution.

Two modes of blockage account for the outward *I–V* relationships of Kir2.1 observed with polyamines

We assumed the following simplified model for the high-affinity mode (Mode 1) and low-affinity mode (Mode 2) of the polyamine block of the Kir2.1 channel:

$$\begin{aligned} &\text{Mode 1: Open state} \underset{\alpha_1}{\overset{[PA]\cdot\beta_1}{\rightleftarrows}} \text{Blocked state 1} \\ &\text{Mode 2: Open state} \underset{\alpha_2}{\overset{[PA]\cdot\beta_2}{\rightleftarrows}} \text{Blocked state 2} \end{aligned} \quad (2)$$

where [PA] is the concentration of spermine or spermidine, and β and α are the voltage-dependent block and unblock rate constants, respectively. According to our hypothesis, the steady-state *G–V* relationship is calculated by the following equation:

$$\frac{G}{G_{max}} = \frac{\phi}{1 + \dfrac{[PA]}{K_{d1(PA)}(V)}} + \frac{1 - \phi}{1 + \dfrac{[PA]}{K_{d2(PA)}(V)}} \quad (3)$$

(Mode 1) (Mode 2),

where ϕ is the maximum value of the fractional conductance generated by the Mode 1 channels (defined as the channels accepting only the Mode 1 block), and $K_{d1(PA)}(V)$ and $K_{d2(PA)}(V)$ are the

spermine; open symbols, spermidine). See text for equations reconstructing $K_{d1(spm)}(V)$, $K_{d1(spd)}(V)$, $K_{d2(spm)}(V)$ and $K_{d2(spd)}(V)$ values. *D*, fractional blockages of Mode 1 (upper panel) and Mode 2 (lower panel) channels by spermine at different voltages, calculated using $K_{d1(spm)}(V)$ and $K_{d2(spm)}(V)$ values, respectively (dotted line, 0.1 μM; dashed line, 1 μM; continuous line, 10 μM). *E*, fractional blockage of currents in Mode 1 (dotted line) and Mode 2 (dashed line) at 5 μM spermine calculated by the model. The proportion of Mode 1 channels to total channels (ϕ) is 0.9. The continuous line indicates the sum of the two fractions. *F*, reconstruction of *G–V* relationships obtained with various concentrations of spermine and spermidine. The continuous lines are G/G_{max} values calculated using eqn (3) with $K_d(V)$ values shown in *C* and ϕ values of 0.9 and 0.75 for the spermine and spermidine data, respectively. Symbols are the mean data values shown in Fig. 2. The top panel illustrates how the sum of conductances generated by Mode 1 (dotted line) and Mode 2 (dashed line) channels reconstructed the *G–V* relationship at 5 μM spermine.

voltage-dependent dissociation constants ($K_d(V)$) of the spermine/spermidine block in Mode 1 and Mode 2, respectively. The ϕ value is equivalent to the proportion of Mode 1 channels to total channels if the unit conductances of the Mode 1 channels and Mode 2 channels (the channels accepting only the Mode 2 block) are the same.

To examine whether or not the above hypothesis is feasible, we obtained $K_{d1(PA)}(V)$ and $K_{d2(PA)}(V)$ values that would be able to explain the data. To gain estimates of the $K_{d1(PA)}(V)$ values of the spermine (spm) and spermidine (spd) block ($K_{d1(spm)}(V)$ and $K_{d1(spd)}(V)$), dose–response relationships were analysed in the voltage range around 0 mV, where the *G*–*V* relationships showed a strong voltage dependence (Fig. 3*A*). The $K_{d2(PA)}(V)$ values of the spermine and spermidine block ($K_{d2(spm)}(V)$ and $K_{d2(spd)}(V)$) were estimated from dose–response relationships at voltages between +40 and +70 mV, normalized with respect to the maximum conductance value in this voltage range (Fig. 3*B*), since conductances in this voltage range appeared to be generated mostly by the Mode 2 channels at the examined concentrations (Fig. 2, lower panels). The K_d values obtained from the dose–response relationships decreased exponentially as the voltage became more positive (Fig. 3*C*, symbols). Based on these values, we determined the voltage dependences of $K_{d1(spm)}(V)$, $K_{d1(spd)}(V)$, $K_{d2(spm)}(V)$, and $K_{d2(spd)}(V)$ (Fig. 3*C*, lines) and the ϕ values of 0.9 for the spermine block and 0.75 for the spermidine block, which resulted in good fits of the *G*–*V* relationships with eqn (3), except for the decrease in the conductances at the negative voltages observed with 10 μM spermine or 30–100 μM spermidine (Fig. 3*F*). The $K_{d1(spm)}(V)$, $K_{d1(spd)}(V)$, $K_{d2(spm)}(V)$ and $K_{d2(spd)}(V)$ values could be expressed using the following equation (Woodhull, 1973):

$$K_d(V) = K_d(0)\exp(-z'FV/RT) \tag{4}$$

where *F*, *R*, and *T* are the thermodynamic constants, z' is the effective valency of the blockage, *V* is the membrane potential in millivolts, and $K_d(0)$ is the K_d value at 0 mV. The $K_d(0)$ and $RT/z'F$ values were 0.7 μM and 4.8 mV for $K_{d1(spm)}(V)$, 40 μM and 9.1 mV for $K_{d2(spm)}(V)$, 10 μM and 5.9 mV for $K_{d1(spd)}(V)$, and 300 μM and 9.2 mV for $K_{d2(spd)}(V)$, respectively. The upper panel of Fig. 3*F* demonstrates how the sum of conductances generated by the Mode 1 and Mode 2 channels reconstructed the *G*–*V* relationships. When eqn (4) is substituted into eqn (3), the *G*–*V* relationship at 5 μM spermine is expressed by the sum of two Boltzmann relations as follows:

$$\frac{G}{G_{max}} = \underbrace{\frac{0.9}{1+\exp\left((V-(-9.4))/4.8\right)}}_{\text{(Mode 1)}} + \underbrace{\frac{0.1}{1+\exp\left((V-18.9)/9.1\right)}}_{\text{(Mode 2)}} \tag{5}$$

Figure 3*D* illustrates the fractional blockages of the Mode 1 and Mode 2 channels by 0.1–10 μM spermine calculated at different voltages. The potency and voltage dependence of the polyamine block in Mode 2 are weaker than those in Mode 1. In the case where the Mode 1 and Mode 2 channels coexist with the ϕ value of 0.9, the fractional blockage of the currents in each mode in the presence of 5 μM spermine is calculated as shown in Fig. 3*E*. The fractional block in Mode 1 saturates at voltages more positive than ~20 mV, whereas the fractional block in Mode 2 increases at voltages more positive than ~0 mV, causing the complete blockage of currents at voltages more positive than ~60 mV.

Figure 4*A* and *B* shows the *I*–*V* relationships at various spermine/spermidine concentrations, reconstructed using calculated G/G_{max} values. The model reproduced the outward *I*–*V* relationships obtained in the experiments (Fig. 1*B*). With either 5–10 μM spermine or 10–100 μM spermidine, the outward *I*–*V* relationships of Kir2.1 were similar to the steady-state outward *I*–*V* relationship of I_{K1}. At these concentrations, the majority of the outward currents were reconstructed by the Mode 2 channels (e.g. Fig. 4*C*).

Two components in the time course of the inward currents observed in the presence of spermine

The inward currents of Kir2.1 observed by the whole-cell recordings exhibited an exponential phase following a virtually instantaneous increase upon hyperpolarization, similar to that obtained for I_{K1}, and the exponential phase was considered to reflect the relief from the spermine block of the channel (Ishihara *et al.* 1996). However, if two modes of blockage are indeed involved in the polyamine block of Kir2.1, the time course of the inward currents reflecting the relief from the polyamine block may contain two components. In the experiment shown in Fig. 5, we analysed the inward tail currents observed following test pulses in the presence of 5 μM spermine. This analysis was not performed with spermidine, since the relief from the spermidine block of the Kir2.1 channel was rapid, thus rendering it difficult to analyse its time dependence (Ishihara *et al.* 1996; Xie *et al.* 2002). Following

test pulses within a voltage range more negative than +20 mV (−15, −10, −5 and +15 mV in Fig. 5*A*, left column), the time-dependent fraction of the inward tail currents at −30 mV increased as the voltage during the test pulse became more positive (top panel). The majority of the time-dependent components could be fitted by a single exponential function with the same time constant of 0.74 ms (middle panel), and the amplitude of this exponential component (I_{Time}) increased, as demonstrated by the theoretical curves (bottom panel). Following test pulses at voltages more positive than +20 mV (+20, +40, +60 and +80 mV in Fig. 5*A*, right column), the amplitude of the exponential component saturated (top and middle panels) and failed to explain the whole inward current amplitude at −30 mV (I_{Max}; bottom panel). It should be noted that there were no outward currents corresponding to the instantaneous currents at −30 mV during the preceding test pulses (top right panel).

Figure 5*B* shows the relationship between the voltage of the test pulses and the exponential fraction of the inward tail currents (I_{Time}/I_{Max}; •), indicating the fraction of the blockage at the test potentials that was relieved with an exponential time course at −30 mV. This relationship was found to be similar to that of the fractional block in Mode 1, calculated by the model (Fig. 3*E*), because the exponential fraction approached a limit at a submaximal level in the voltage range more positive than ∼20 mV. The voltage dependence of the exponential fraction could be approximated by a single Boltzmann relation (continuous line in Fig. 5*B*; $V_h = -9.8$ mV, $s = -5.7$ mV, maximum level = 0.84), which was similar to the Boltzmann relation describing the blockage of the Mode 1 channel by 5 μM spermine (eqn (5)). On the other hand, in the positive voltage range, the fractional block of currents at the end of the test pulses, estimated from the conductance measurements ($1 - G/G_{max}$; ○ in Fig. 5*B*), was evidently larger than the fraction of the blockage that was relieved with an exponential time course (•). This finding clearly indicated that the time course of the relief from the spermine block consisted of not only an exponential component but also a much faster component (△ in Fig. 5*B*). The virtually instantaneous fraction (△) increased in the voltage range between 0 mV and ∼60 mV, which was analogous to the voltage dependence of the fractional block in Mode 2, calculated by the model (Fig. 3*E*). These findings suggested that the exponential component and the instantaneous component reflect the time courses of the relief from the spermine block in Mode 1 and Mode 2, respectively. Essentially the same findings were obtained in analyses of the currents obtained from different patches in the presence of 1 or 5 μM spermine (data not shown). These results supported the model we employed to explain the *G*–*V* relationships of Kir2.1, obtained in the presence of polyamines.

Kir2.1 currents under conditions in which spermine and spermidine coexist

Although the outward *I*–*V* relationships of Kir2.1 currents obtained in the presence of either ∼5 μM spermine or ∼30 μM spermidine alone (Fig. 1*B*) were similar to that of I_{K1} in the steady state, both species of polyamine coexist in the cytoplasm. Next, we examined the outward *I*–*V* relationships of Kir2.1 obtained under conditions in which spermidine coexisted with spermine (Fig. 6*A*). When 10 or 30 μM spermidine coexisted with 5 μM spermine,

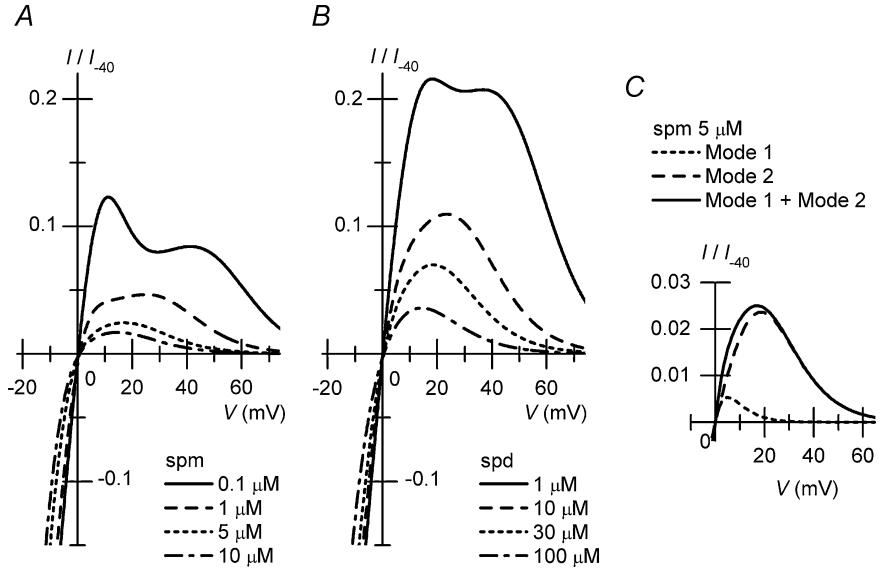

Figure 4. Reconstruction of *I–V* relationships of Kir2.1 in the presence of cytoplasmic polyamines
A, calculations of *I–V* relationships in the presence of spermine (spm; continuous line, 0.1 μM; dashed line, 1 μM; dotted line, 5 μM; dot–dashed line, 10 μM). Compare these relationships with those shown in Fig. 1*Ba*. *B*, calculations of *I–V* relationships in the presence of spermidine (spd; continuous line, 1 μM; dashed line, 10 μM; dotted line, 30 μM; dot–dashed line, 100 μM). Compare these relationships with those shown in Fig. 1*Bb*. *C*, amplitudes of the outward currents generated by Mode 1 channels (dotted line) and Mode 2 channels (dashed line) in the presence of 5 μM spermine. The continuous line is the sum of the two components.

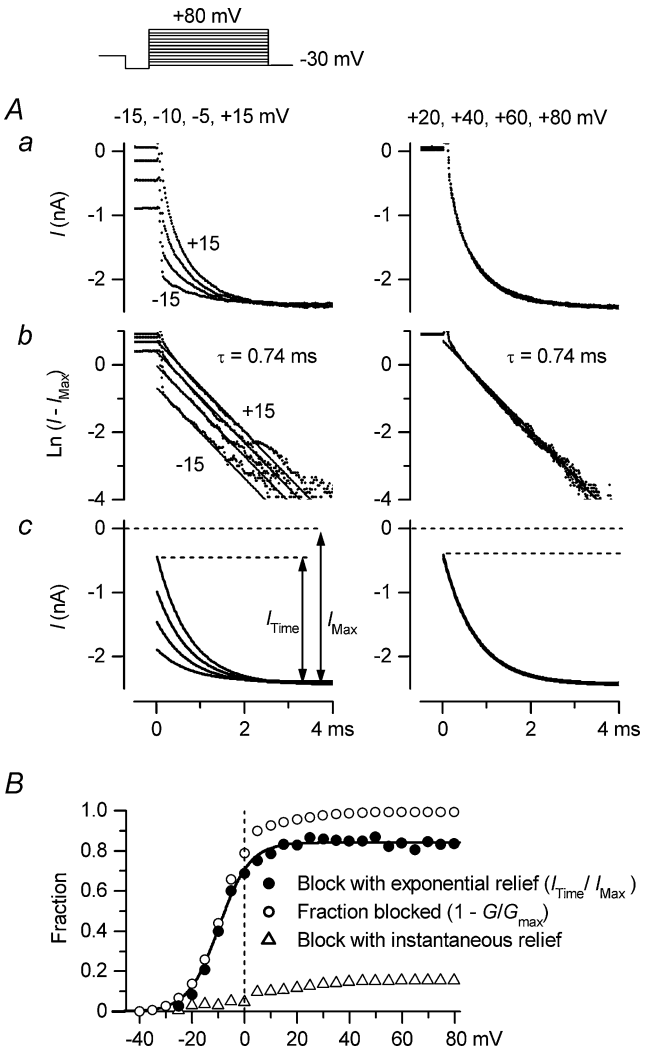

Figure 5. Two components of the inward currents of Kir2.1 observed with 5 μm spermine

A, analysis of inward tail currents at −30 mV observed following 100 ms test pulses applied after a hyperpolarizing prepulse. Voltages of test pulses were −15, −10, −5 and +15 mV in the left column, and +20, +40, +60 and +80 mV in the right column. *Aa*, original currents plotted *versus* time after applying the voltage step to −30 mV. *Ab*, natural logarithm of the difference between amplitudes of the original current and the maximum inward current (I_{Max}). Straight lines show fittings with a single-exponential function (time constant, 0.74 ms). *Ac*, exponential components of inward tail currents at −30 mV (I_{Time}) reconstructed using the fitted exponentials. *B*, exponential fraction of the inward tail currents at −30 mV (I_{Time}/I_{Max}; ●), indicating the fraction of the block that is relieved with an exponential time course, plotted against the voltage of test pulses. Data were obtained from the experiment shown in *A*. The continuous line shows a fit with the Boltzmann relation ($V_h = -9.8$ mV, $s = -5.7$ mV). Also shown are the fractional block of currents at the end of the test pulses (○), obtained as $1 - G/G_{max}$, and the fraction of block that is relieved with a virtually instantaneous time course at −30 mV (△), obtained as the difference between the fraction blocked (○) and the fraction of block with an exponential relief calculated by the fitted Boltzmann relation.

the amplitude of the outward currents decreased slightly throughout the entire voltage range examined (left panel). However, when 2, 5, or 30 μM spermidine coexisted with 1 μM spermine, the amplitude of the outward currents increased at certain voltages (around +20 mV), which caused the crossover of the outward *I–V* relationships obtained in the presence and absence of spermidine (centre and right panels). Moreover, the peak amplitude of the outward currents observed with 1 μM spermine + 5 μM spermidine was larger than that with 1 μM spermine + 2 μM spermidine.

If spermine and spermidine compete to block the Mode 1 and Mode 2 channels, the steady-state *G–V* relationship is calculated by the following equation:

$$\frac{G}{G_{max}} = \frac{\phi}{1 + \dfrac{[spm]}{K_{d1(spm)}(V)} + \dfrac{[spd]}{K_{d1(spd)}(V)}} \quad \text{(Mode 1)}$$

$$+ \frac{1-\phi}{1 + \dfrac{[spm]}{K_{d2(spm)}(V)} + \dfrac{[spd]}{K_{d2(spd)}(V)}} \quad \text{(Mode 2)} \qquad (6)$$

In the presence of either 0.1–10 μM spermine or 1–100 μM spermidine alone, $G(I)$–V relationships could be well explained using eqn (3) (or eqn (6)) with the $K_d(V)$ values shown in Fig. 3*C* and a ϕ value (the fraction of Mode 1 channels) of 0.9 or 0.75, respectively (Figs 3*F* and 4). When spermidine coexisted with spermine, the outward *I–V* relationships were found to be well reconstructed with the same $K_d(V)$ values by reducing the ϕ value, to lie below 0.9 and closer to 0.75, as the concentration of spermidine increased (Fig. 6*B* and *D*). For example, using a ϕ value of 0.89 for 1 μM spermine + 2 μM spermidine, 0.87 for 1 μM spermine + 5 μM spermidine, and 0.81 for 1 μM spermine + 30 μM spermidine, the increase in the amplitude of the outward currents observed at around +20 mV could be well reproduced by the increase in the amplitude of the outward currents through the Mode 2 channels (Fig. 6*C*). This finding indicated that an increase in the spermidine concentration in the copresence of spermine might have two opposing effects on the outward currents: a decrease in the amplitude of the outward current due to an increase in the blockage of the Mode 1 and Mode 2 channels, and an increase in the amplitude of the outward current due to an increase in the fraction of the Mode 2 channels.

The above findings suggest that the probability of the Kir2.1 channel existing in either of the two conformational states that allow different modes of blockage (Mode 1

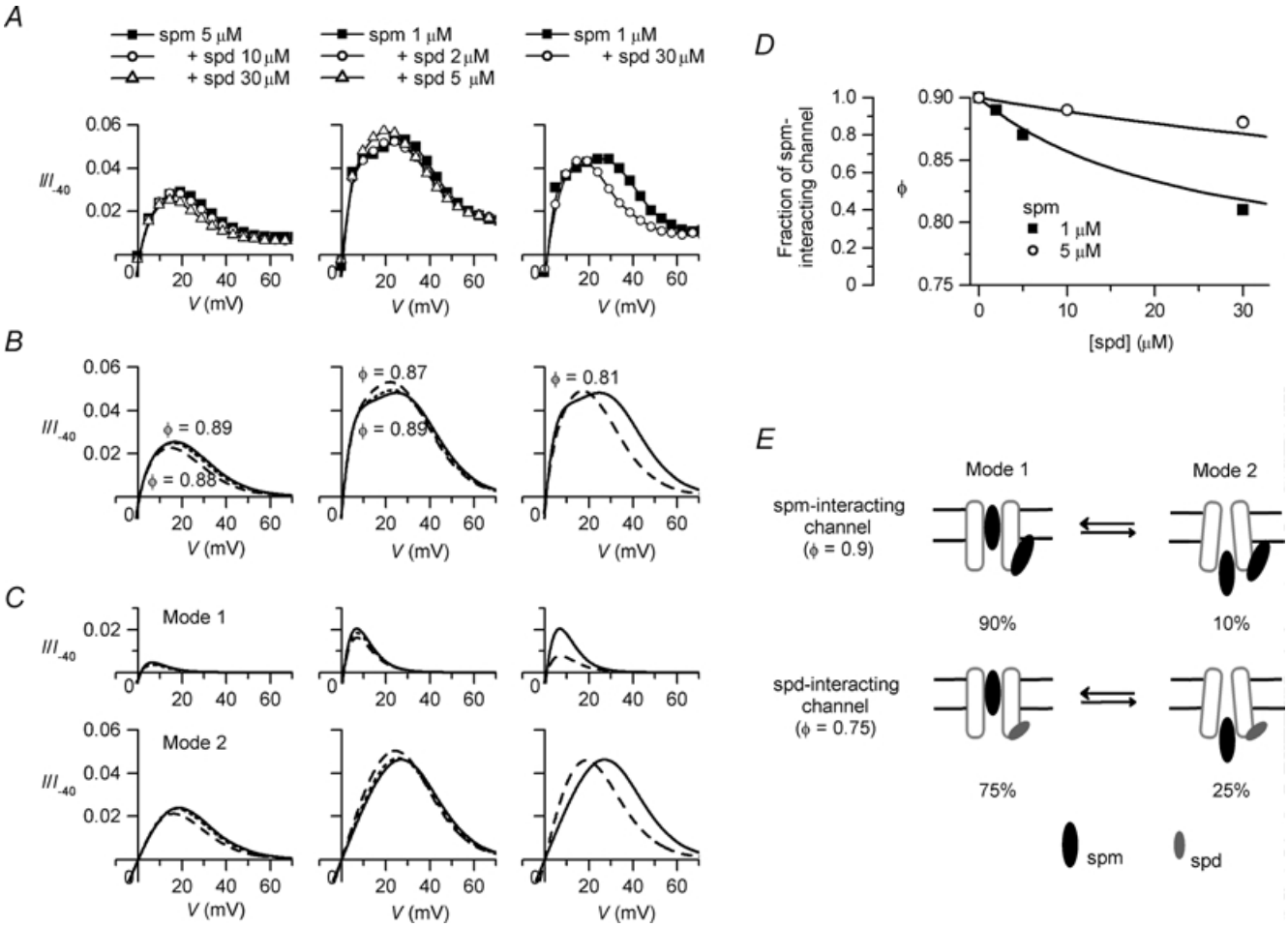

Figure 6. Outward *I–V* relationships of Kir2.1 under conditions in which spermine and spermidine coexisted

A, outward *I–V* relationships obtained from experiments. Left, 5 μM spermine (spm) (■), 5 μM spermine + 10 μM spermidine (spd) (○), 5 μM spermine + 30 μM spermidine (△); centre, 1 μM spermine (■), 1 μM spermine + 2 μM spermidine (○), 1 μM spermine + 5 μM spermidine (△); right, 1 μM spermine (■), 1 μM spermine + 30 μM spermidine (○). Data plotted in the same panel were obtained from the same patch. Current amplitudes were normalized with respect to that at −40 mV obtained with spermine alone. *B*, reconstruction of outward *I–V* relationships. Left, 5 μM spermine (continuous line), 5 μM spermine + 10 μM spermidine (dotted line), 5 μM spermine + 30 μM spermidine (dashed line); centre, 1 μM spermine (continuous line), 1 μM spermine + 2 μM spermidine (dotted line), 1 μM spermine + 5 μM spermidine (dashed line); right, 1 μM spermine (continuous line), 1 μM spermine + 30 μM spermidine (dashed line). Calculations were performed using eqn (6) with $K_d(V)$ values shown in Fig. 3*C*. Values of ϕ in the copresence of spermine and spermidine are depicted near each relationship and in the text. *C*, outward *I–V* relationships of Mode 1 channels (upper row) and Mode 2 channels (lower row) calculated by the model. *D*, relationship between the concentration of spermidine coexisting with spermine (■, 1 μM; ○, 5 μM) and the fraction of Mode 1 channels (ϕ) that accounted for the outward *I–V* relationships. Values of ϕ are also shown in relation to the fraction of the spermine-interacting channels calculated by assuming that the probability of the channel existing in the state that allows the Mode 1 block is 0.9 for spermine-interacting channels and 0.75 for spermidine-interacting channels. The continuous lines are the fraction of the spermine-interacting channels calculated by ([spermine]/0.002)/(1 + [spermine]/0.002 + [spermidine]/0.05), where [spermine] and [spermidine] are in micromolar concentrations. *E*, hypothetical mechanism of modification of the ratio of Mode 1 channels to Mode 2 channels by cytoplasmic polyamine. Interaction of spermine or spermidine with the Kir2.1 channel at an intracellular site may change the equilibrium of the two conformational states of the channel allowing different modes of blockage.

state and Mode 2 state) is not fixed, but is altered by the interaction of spermine/spermidine with the channel at an intracellular site (Fig. 6*E*). The finding that the equilibrium of the two states did not notably change in the concentration range between 0.1 and 10 μM for spermine and between 1 and 100 μM for spermidine may be explained if the K_d values of the interaction were much smaller than 0.1 μM with spermine and 1 μM with spermidine. If we assume that the probabilities of the spermine- and spermidine-interacting channels to exist in the Mode 1 state are 0.9 and 0.75, respectively, and that spermidine and spermine compete for interaction with the channel, then the fractions of the spermine- and spermidine-interacting channels can be calculated from the ϕ values (Fig. 6*D*). The fractions of the spermine-interacting channels thus obtained could be explained by assuming that the K_d value of the spermidine–channel interaction is approximately 25-fold larger than that of the spermine–channel interaction. For example, the continuous lines in Fig. 6*D* show the fraction of the spermine-interacting channels, calculated using the K_d values of 0.002 μM and 0.05 μM for the spermine–channel

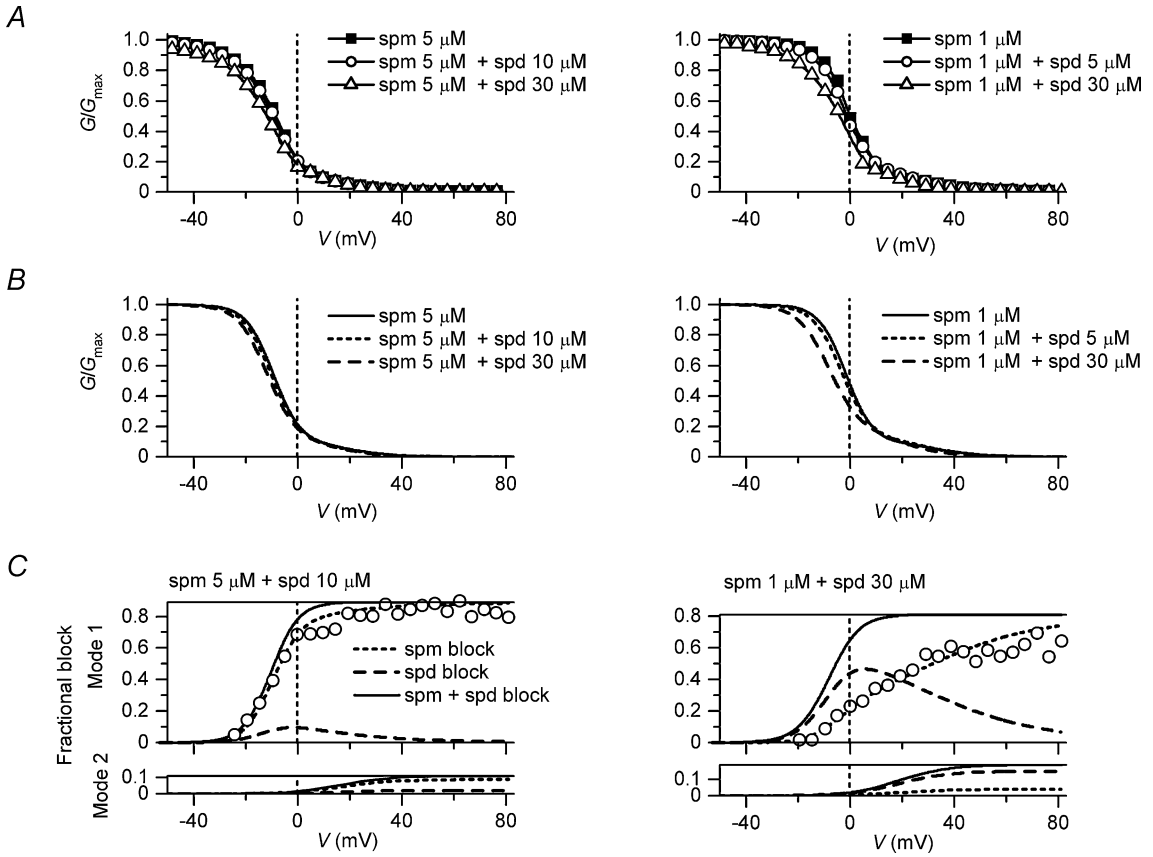

Figure 7. Spermine block and spermidine block of Kir2.1 channels under conditions in which spermine and spermidine coexisted

A, *G–V* relationships obtained from experiments. Left, 5 μM spermine (spm) (■), 5 μM spermine + 10 μM spermidine (spd) (○), 5 μM spermine + 30 μM spermidine (△); right, 1 μM spermine (■), 1 μM spermine + 5 μM spermidine (○), 1 μM spermine + 30 μM spermidine (△). *B*, reconstruction of *G–V* relationships. Left, 5 μM spermine (continuous line), 5 μM spermine + 10 μM spermidine (dotted line), 5 μM spermine + 30 μM spermidine (dashed line); right, 1 μM spermine (continuous line), 1 μM spermine + 5 μM spermidine (dotted line), 1 μM spermine + 30 μM spermidine (dashed line). Calculations were performed using eqn (6) with $K_d(V)$ values shown in Fig. 3*C* and the ϕ values used for the calculations shown in Fig. 6. *C*, fractional block of Mode 1 channels (upper panels) and Mode 2 channels (lower panels) by spermine (dotted line) and spermidine (dashed line) calculated for 5 μM spermine + 10 μM spermidine with a ϕ value of 0.89 (left) and 1 μM spermine + 30 μM spermidine with a ϕ value of 0.81 (right). Continuous lines show the sum of fractional blockages caused by spermine and spermidine. The experimental data showing the relationship between the voltages of test pulses and the exponential fraction of inward tail currents at −30 mV (I_{Time}/I_{Max}, explained in Fig. 5) obtained under each condition are superimposed (○). Data in *A* and *C* were obtained from the same patch.

and spermidine–channel interactions, respectively. By provisionally using these K_d values, the ϕ value is calculated as follows:

$$\phi = \frac{0.9([\text{spm}]/0.002) + 0.75([\text{spd}]/0.05)}{1 + [\text{spm}]/0.002 + [\text{spd}]/0.05} \quad (7)$$

where the concentrations of spermine [spm] and spermidine [spd] are micromolar.

The *G–V* relationships obtained in the copresence of spermine and spermidine (Fig. 7*A*) could be also reproduced by using the ϕ values that were able to reconstruct the outward *I–V* relationships, except for the decrease in the conductances in the negative voltages observed with 30 μM spermidine (Fig. 7*B*). Figure 7*C* illustrates the fractional blockages of Mode 1 channels (upper panels) and Mode 2 channels (lower panels) caused by spermine and spermidine, calculated for 5 μM spermine + 10 μM spermidine (left) and 1 μM spermine + 30 μM spermidine (right). Under both conditions, the voltage dependence of the fraction blocked by spermine of the Mode 1 channels agreed well with the experimental data showing the relationship between the voltage of test pulses and the exponential fraction of the inward tail current at −30 mV (Fig. 7*C*, ○). These findings further justified the use of the model.

Under both conditions, i.e. 5 μM spermine + 10 μM spermidine and 1 μM spermine + 30 μM spermidine, the outward *I–V* relationships were similar to that of I_{K1} (Fig. 6*A*). Under the former condition, the conductances of Mode 2 channels, generating most of the outward currents, were determined by the spermine block, whereas in the latter condition, they were chiefly determined by the spermidine block (Fig. 7*C*, lower panels). Under the latter condition, the spermine block of Mode 1 channels showed a voltage dependence that was much weaker than that observed with spermine alone, because spermidine competed with spermine for blocking Mode 1 channels (Fig. 7*C*, upper right panel, cf. Fig. 5*B*). This weak voltage dependence was clearly different from the steep voltage dependence of the time-dependent gating of I_{K1} (Kurachi, 1985; Tourneur *et al.* 1987; Oliva *et al.* 1990), suggesting that the concentration of spermidine in cardiac cells may not be considerably higher than that of spermine. Thus, it is likely that the amplitude of the outward I_{K1} is chiefly determined by blockage of the Mode 2 channels with around 5–10 μM spermine.

Discussion

We attempted to study the mechanism for generating the outward current of the cardiac I_{K1} using the Kir2.1 channel expressed in human cells. Plotting the *G–V* relationships of Kir2.1 currents obtained with 0.1–10 μM spermine or 10–100 μM spermidine on a semilogarithmic scale (Fig. 2) strongly suggested that the conductances that generated the outward currents of Kir2.1 were the sum of conductances from two types of channels, which were blocked by cytoplasmic polyamines in either the high-affinity mode (Mode 1 channel) or the low-affinity mode (Mode 2 channel). The $K_d(V)$ values of the spermine block and the spermidine block in the respective modes were determined, which could quantitatively account for the outward $G(I)$–V relationships obtained in the presence of different concentrations of spermine and/or spermidine (Figs 3, 4, 6 and 7). The estimated proportion of Mode 1 channels to total channels (ϕ) was 0.9 with 0.1–10 μM spermine alone, 0.75 with 10–100 μM spermidine alone, and between 0.75 and 0.9 when spermine and spermidine coexisted. This finding implied that an interaction of cytoplasmic spermine/spermidine with the channel at an intracellular site affects the equilibrium of the two conformational states of the channel that allow different modes of blockage. If we assume that spermine and spermidine compete for this interaction, the K_d value for the spermidine–channel interaction was calculated to be approximately 25-fold larger than that for the spermine–channel interaction. Our results suggest that the outward I_{K1} may largely flow through a small population of channels (Mode 2 channels) that are less sensitive to the polyamine block. Polyamines may regulate the amplitude of the outward I_{K1} by not only blocking the channel currents but also by changing the ratio of the Mode 1 and Mode 2 channels.

Experimental conditions

The expression vector pCXN2 (Niwa *et al.* 1991) allowed such a high level of Kir2.1 channel expression in HEK 293T cells that the macroscopic currents could be recorded from patch membranes using pipette electrodes with the usual tip diameter (Kubo & Murata, 2001). The *G–V* relationship of the Kir2.1 channel expressed in L cells, obtained with 1 μM spermine (Ishihara, 1997), and that expressed in *Xenopus* oocytes, obtained with 100 μM spermidine (Yang *et al.* 1995), were nearly identical to the results in this study. Thus, a high expression of the channel did not influence the sensitivity of the channel to cytoplasmic polyamines.

Even long after exposing the patch membranes to the Mg^{2+}-free, polyamine-free cytoplasmic solution, a slow decline in the outward currents was generally observed during long depolarizing pulses (Fig. 1*Aa*), as previously

reported (Lopatin *et al.* 1995; Shieh *et al.* 1996). Recent studies, using the *Xenopus* oocyte expression system, have shown that this 'spontaneous gating' can be largely eliminated by using a phosphate buffer instead of Hepes and replacing EGTA with EDTA (Guo & Lu, 2000*b*, 2002). Although we could confirm that this spontaneous gating was significantly slower and less pronounced when a phosphate buffer was used, its complete removal was still unusual, as has been recently shown in the single-channel recordings of Kir2.1 (Matsuda *et al.* 2003). Since the blockage of Kir2.1 currents by polyamines at the examined concentrations was much more rapid and greater than the above-mentioned spontaneous gating, we considered that the gating scarcely interfered with the analysis of the currents in the present study.

Polyamine block of the strong inward rectifier K^+ channels, Kir2, generating two phases in *G–V* relationships

The polyamine block of the strong inward rectifier K^+ channels is not well understood because it shows complex features that are different in distinct concentration ranges (Lopatin *et al.* 1995; Guo & Lu, 2000*a*; Xie *et al.* 2002). In an analysis of the blockage of the inward currents of the Kir2.3 channel using high concentrations of polyamines (25–500 μM spermine), Lopatin *et al.* (1995) were the first to demonstrate that the polyamine block has two components: a type of blockage showing a weak voltage dependence and an instantaneous time course ('a shallow component') and another type of blockage exhibiting a strong voltage dependence with time-dependent kinetics.

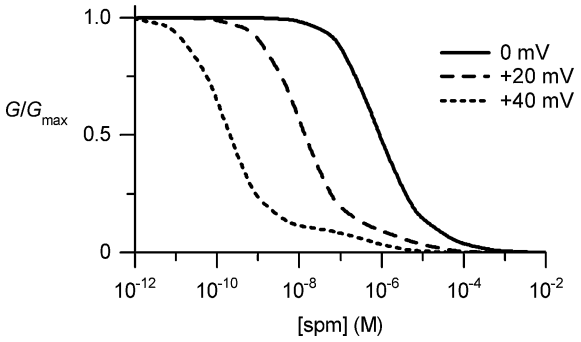

Figure 8. Reconstructed dose–response relationships of the spermine block of the Kir2.1 channel at 0, +20 and +40 mV
These relationships were calculated using eqn (3) with a ϕ value of 0.9 and the $K_{d1(spm)}(V)$ and $K_{d2(spm)}(V)$ values shown in Fig. 3*C*. The relationship at +40 mV shows two phases, as has been reported (Yang *et al.* 1995). According to our view, the hump of conductances observed at higher concentrations is generated by the channels showing lower sensitivity to spermine.

The former component, which we also observed in the inward currents with relatively high concentrations of polyamines (Fig. 2), was recently attributed to a decrease in unit-channel conductance caused by the binding of polyamines to surface charges at the inner vestibule of the channel (Xie *et al.* 2002). Although this shallow component of the polyamine block may also affect the outward currents that flow in the presence of lower concentrations of polyamines, it does not readily account for the mechanism that generates extra conductances. Therefore, this effect was not considered in the present study.

Yang *et al.* (1995) demonstrated that the dose–response relationships of the polyamine block of Kir2.1 analysed at +40 mV with symmetrical 140 mM $[K^+]$ were fitted by the sum of two Hill equations (eqn (3) in this study). The K_{d1} and K_{d2} values at +40 mV and the maximum fractional conductances of the two channel populations we obtained (0.16 nM (0.9) and 0.49 μM (0.1) for spermine, and 11 nM (0.75) and 3.9 μM (0.25) for spermidine; maximum fractional conductance in parentheses) were similar to those reported by Yang *et al.* (0.9 nM (0.86) and 0.61 μM (0.14) for spermine, 8 nM (0.7) and 2.87 μM (0.3) for spermidine). Thus, when we reconstructed the dose–response relationship of the spermine block at +40 mV (Fig. 8), a hump of conductances appeared in the higher concentration range, as demonstrated by Yang *et al.* Since the channels expressed from a cloned gene are expected to be homogeneous, Yang *et al.* instead speculated that the K_d value for a single type of channel may have increased with higher concentrations of the blockers. They suggested that the channel might accommodate more than one blocking particle, which may in turn lead to negative cooperativity due to mechanisms such as electrostatic repulsion between the blockers. Indeed, they later provided evidence that the Kir2.1 channel can simultaneously accommodate three polyamines or Mg^{2+} in the wide inner pore of the channel (Lu *et al.* 1999). However, we found that the extra conductances, which may be generated by the repulsion between the blockers inside a channel, were larger with lower concentrations of polyamines (Fig. 2, lower panels). Further, the dose–response relationship obtained at 0 mV could be approximated by a single Hill equation (Fig. 3*A*; see also Xie *et al.* 2002), which differs as regards the observation of the dose–response relationship obtained at +40 mV (Fig. 8). These findings cannot be explained by the repulsion hypothesis unless we further hypothesize, for example, that the channel undergoes a voltage-dependent conformational change, which would then allow it to accommodate more than one blocking particle in the positive voltage range. On the other hand,

if we hypothesize two types of channels that are blocked by polyamines in distinct modes (with different voltage dependencies and potencies), various shapes of $G(I)$–V relationships observed with different concentrations of polyamines could be quantitatively accounted for (Figs 3, 4, 6 and 7). The dose–response relationship at 0 mV was also reconstructed (Fig. 8).

More recently, Guo & Lu (2000*a*) studied the polyamine block of Kir2.1 with low concentrations of polyamines (0.03–1 μM spermine/spermidine) and showed that the outward I–V relationships exhibit a double-hump shape in the presence of polyamines, as shown in the present study (Fig. 1*B*). In their study, the phenomenon was explained essentially by the following model, which assumes that polyamines block the channel by inducing two blocked states in which the polyamines are bound with different affinities. Thus, their view is basically in agreement with that of Yang *et al.* (1995) and our own in this respect; however, it differs from our view point with regard to their suggestion that two types of blockage occur in a single type of channel:

$$\text{Blocked state 1} \underset{[\text{PA}]\cdot\beta_1}{\overset{\alpha_1}{\rightleftarrows}} \text{Open state} \underset{\alpha_2}{\overset{[\text{PA}]\cdot\beta_2}{\rightleftarrows}} \text{Blocked state 2} \quad (8)$$

In this model, the conductance is calculated by the following equation:

$$\frac{G}{G_{\max}} = \frac{1}{1 + \dfrac{[\text{PA}]}{K_{\text{d1(PA)}}(V)} + \dfrac{[\text{PA}]}{K_{\text{d2(PA)}}(V)}}, \quad (9)$$

where $K_{\text{d1(PA)}}(V)$ and $K_{\text{d2(PA)}}(V)$ are the K_{d} values of the blockage at the high- and low-affinity sites of the channel, respectively. This model may also apply to the channel that has two polyamine binding sites, and the bindings of polyamine to the two sites are mutually exclusive. If K_{d} values show a monotonic voltage dependence such as those shown in Fig. 3*C*, the extra conductances in the G–V relationships (Fig. 2, lower panels) cannot be reconstructed by eqn (9). Guo and Lu assumed that the $K_{\text{d1(PA)}}$ values become larger than the $K_{\text{d2(PA)}}$ values at positive voltages, such as those shown in Fig. 9*Aa*, and argued that this phenomenon may occur if the polyamines traverse the pore at positive voltages, thus relieving the blockage. In this case, the reaction between the channel and the polyamine at the high-affinity site may be described as follows:

$$\text{X1} + \text{PA}_{\text{IN}} \underset{\alpha_1}{\overset{\beta_1}{\rightleftarrows}} \text{X1}\cdot\text{PA} \xrightarrow{\kappa} \text{X1} + \text{PA}_{\text{OUT}} \quad (10)$$

where X1 is the high-affinity site that binds to the polyamine (X1·PA); PA_{IN} and PA_{OUT} are the polyamines existing inside and outside the channel, respectively; and κ is the voltage-dependent rate constant. The apparent dissociation constant $K_{\text{d1(PA)}}(V)$ is $(\alpha_1 + \kappa)/\beta_1$, and it approximates to κ/β_1 if κ is large compared with α_1. When the extra conductances in the G–V relationships were simulated using eqn (9) with this assumption (Fig. 9*Ab*), $K_{\text{d1(spm)}}$ values in the positive voltage range, which may represent κ/β_1, significantly varied at different spermine concentrations (Fig. 9*Aa*). When the same set of $K_{\text{d1(spm)}}(V)$ values was used to calculate the relationships at different spermine concentrations, the amplitude of the extra conductances greatly varied (Fig. 9*B*), which was obviously different from our finding that the maximum values of the extra conductances were similar in the concentration range between 0.1 and 10 μM (Fig. 2, lower panels). Furthermore, the blockage at the low-affinity site, calculated by model (8), significantly increased at the expense of that at the high-affinity site in the positive voltage range (Fig. 9*C*). When we analysed the relationship between the voltage of the test pulses and the exponential fraction of the inward tail currents (Fig. 5*B*), which may indicate the fractional block at the high-affinity site in model (8), the exponential component always approached a limit at a submaximal level in the positive voltage range. This finding was consistent with model (2), which considers two types of channels that are blocked by polyamines in distinct modes (Fig. 3*E*).

The mechanism that leads to two types of blockage

The voltage dependences of the spermine/spermidine block in Mode 1 were steeper than those in Mode 2 (Fig. 3*C*). Thus, polyamines may move deeper into the pore in the case of the Mode 1 block. It has been demonstrated that polyamines plug the Kir2.1 channel pore at several distinct sites: at D172 in the M2 transmembrane domain (Stanfield *et al.* 1994*b*; Wible *et al.* 1994) and at glutamate residues E224 and E299 in the C-terminal region (Taglialatela *et al.* 1995; Yang *et al.* 1995; Kubo & Murata, 2001). It has been shown that the D172N mutant channel not only lacks the time-dependent gating mechanism (Stanfield *et al.* 1994*b*; Wible *et al.* 1994), but also shows G–V relationships fitted with a single Boltzmann relation in the presence of polyamines (Yang *et al.* 1995). Furthermore, the polyamine sensitivity of D172N channel is comparable to that of the Mode 2 channel obtained in this study or that of the wild-type channel at the low-affinity site (Yang *et al.* 1995). These findings may suggest that D172 forms the spermine-binding site for the Mode 1 block, and that the polyamine-binding site in the D172N channel

(which is not fully explained by E224 and E299; Kubo & Murata, 2001) is nearly the same as the site for the Mode 2 block.

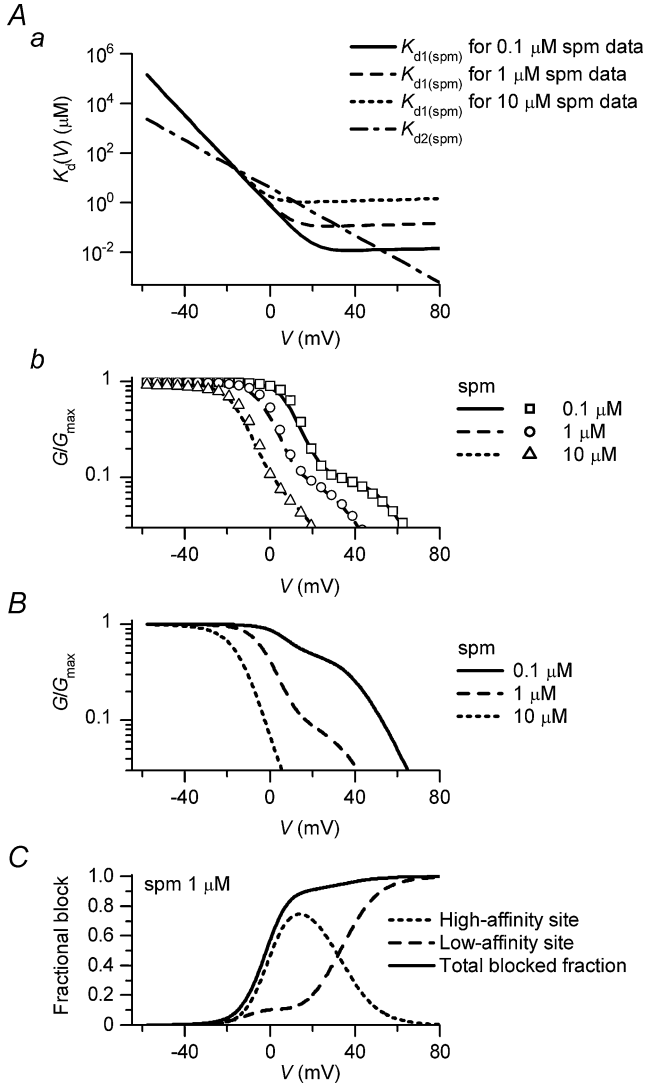

Figure 9. Examination of the model of the polyamine block incorporating two blocked states in a single type of channel
A, fits of *G–V* relationships obtained with 0.1, 1 and 10 μM spermine. *Aa*, $K_d(V)$ values of the spermine block at the high-affinity site ($K_{d1(spm)}(V)$) and the low-affinity site ($K_{d2(spm)}(V)$) that could fit the data. $K_{d1(spm)}(V)$ values were different for 0.1 μM (continuous line), 1 μM (dashed line) and 10 μM (dotted line) spermine in the positive voltage range. $K_{d1(spm)}(V)$ determined for the 1 μM spermine data was calculated by $0.8\exp(-V/4.8) + 0.1\exp(V/200)$ (in μM). $K_{d2(spm)}(V)$ was calculated by $4\exp(-V/9.1)$ (in μM) for all spermine concentrations (dot–dashed line). *Ab*, *G–V* relationships calculated by eqn (9) using the $K_{d1(spm)}(V)$ and $K_{d2(spm)}(V)$ values shown in *A*. Experimental data shown by symbols (□, 0.1 μM; ○, 1 μM; △, 10 μM) are the same as those shown in Fig. 2. *B*, *G–V* relationships calculated at 0.1, 1 and 10 μM spermine using $K_{d1(spm)}(V)$ determined for the 1 μM spermine data. *C*, fractional blockage of currents at the high-affinity site (dotted line) and the low-affinity site (dashed line) calculated at 1 μM spermine. The continuous line indicates the sum of the two fractions.

There may be two types of Kir channels that exhibit different sensitivities to the polyamine block. Indeed, it has been demonstrated by the single-channel analysis that there are Kir2.1 channels showing different sensitivities to the external Cs^+ block (Picones *et al.* 2001). The pore structure of the Kir channel may be flexible to some extent, such that the channel undergoes transitions between the two conformational states, which allows the blockers to plug the pore at different sites. Our results suggest that the equilibrium between the two conformations is affected by the interaction of polyamines with the channel at an intracellular site (Fig. 6*E*). Thus, polyamines themselves may change the sensitivity of the channel to the polyamine block. The mechanisms underlying the two types of blockage need to be further examined in the future.

Suggested mechanisms of the outward I_{K1}

In this study, we focused on the mechanism that generates the sustained flow of the outward I_{K1} in the voltage range near V_{rev} (below V_{rev} + ~60 mV). It is known that the strong inward rectification of I_{K1} is primarily caused by a time-dependent gating mechanism operating at around V_{rev}. According to the present study, this time-dependent gating is presumably caused by the spermine block of the Mode 1 channels and its relief. When the *I–V* relationship of I_{K1} was reconstructed using the parameter of the time-dependent gating, the voltage range in which the outward currents flowed was much narrower (below V_{rev} + ~30 mV; Kurachi, 1985; Ishihara *et al.* 1989; Oliva *et al.* 1990) than the range in which the outward I_{K1} actually took place, as in the case of the outward *I–V* relationship of Mode 1 channels reconstructed at 5 μM spermine (Fig. 4*C*). We concluded that there is another population of channels (Mode 2 channels) that generate most of the outward I_{K1}. Our finding that the fraction of Mode 2 channels is changeable might be of physiological importance in regulating the amplitude of the outward I_{K1}.

The present results indicate that the concentration of spermidine near the I_{K1} channel may not be considerably higher than that of spermine, since the time-dependent gating of the Kir2.1 channel lost its steep voltage dependence with an excess amount of spermidine (Fig. 7*C*). Accordingly, it is strongly suggested that the blockage of channels by spermine primarily determines the outward *I–V* relationships of both Mode 1 and Mode 2 channels of I_{K1}. Assuming that the I_{K1} and Kir2.1 channels show similar sensitivities to the polyamine block, the free spermine concentration in the vicinity of the I_{K1} channel might be approximately 5–10 μM.

It should be noted that a transient component appears in the outward currents of both the I_{K1} and Kir2.1 channels during the depolarizing and repolarizing pulses when Mg^{2+} coexists with polyamines in the cytoplasm (Ishihara *et al.* 1996; Ishihara & Ehara, 1998). This outward transient component flows during the repolarization of the cardiac action potentials (Ishihara *et al.* 2002). According to our present view, these results can be interpreted to indicate that the decay of the transients coincided with the increase in the spermine block of the Mode 1 channels. Thus, the Mg^{2+} block of the Mode 1 channels may generate the transient currents. The steady-state outward *I–V* relationship of I_{K1} is not significantly affected by cytoplasmic Mg^{2+}. This may be explained if the sensitivity of the Mode 2 channel to the Mg^{2+} block is low. The mechanism of the Mg^{2+} block of the strong inward rectifiers with respect to the two populations of channels exhibiting distinct affinities to cytoplasmic blockers is currently being investigated.

References

Fabiato A & Fabiato F (1979). Calculator programs for computing the composition of the solutions containing multiple metals and ligands used for experiments in skinned muscle cells. *J Physiol Paris* **75**, 463–505.

Fakler B, Brandle U, Glowatzki E, Weidemann S, Zenner H-P & Ruppersberg JP (1995). Strong voltage-dependent inward rectification of inward rectifier K^+ channels is caused by intracellular spermine. *Cell* **80**, 149–154.

Ficker E, Taglialatela M, Wible BA, Henley CM & Brown AM (1994). Spermine and spermidine as gating molecules for inward rectifier K^+ channels. *Science* **266**, 1068–1072.

Giles WR & Imaizumi Y (1988). Comparison of potassium currents in rabbit atrial and ventricular cells. *J Physiol* **405**, 123–145.

Guo D & Lu Z (2000*a*). Mechanism of IRK1 channel block by intracellular polyamines. *J Gen Physiol* **115**, 799–813.

Guo D & Lu Z (2000*b*). Pore block versus intrinsic gating in the mechanism of inward rectification in strongly rectifying IRK1 channels. *J Gen Physiol* **116**, 561–568.

Guo D & Lu Z (2002). IRK1 inward rectifier K^+ channels exhibit no intrinsic rectification. *J Gen Physiol* **120**, 539–551.

Hagiwara S, Miyazaki S & Rosenthal NP (1976). Potassium current and the effect of cesium on this current during anomalous rectification of the egg cell membrane of a starfish. *J Gen Physiol* **67**, 621–638.

Hamill OP, Marty A, Neher E, Sakmann B & Sigworth FJ (1981). Improved patch-clamp techniques for high-resolution current recording from cells and cell-free membrane patches. *Pflugers Arch* **391**, 85–100.

He Y, Kashiwagi K, Fukuchi J, Terao K, Shirahata A & Igarashi K (1993). Correlation between the inhibition of cell growth by accumulated polyamines and the decrease of magnesium and ATP. *Eur J Biochem* **217**, 89–96.

Ishihara K (1997). Time-dependent outward currents through the inward rectifier potassium channel IRK1. The role of weak blocking molecules. *J Gen Physiol* **109**, 229–243.

Ishihara K & Ehara T (1998). A repolarization-induced transient increase in the outward current of the inward rectifier K^+ channel in guinea-pig cardiac myocytes. *J Physiol* **510**, 755–771.

Ishihara K, Hiraoka M & Ochi R (1996). The tetravalent organic cation spermine causes the gating of the IRK1 channel expressed in murine fibroblast cells. *J Physiol* **491**, 367–381.

Ishihara K, Mitsuiye T, Noma A & Takano M (1989). The Mg^{2+} block and intrinsic gating underlying inward rectification of the K^+ current in guinea-pig cardiac myocytes. *J Physiol* **419**, 297–320.

Ishihara K, Yan D-H, Yamamoto S & Ehara T (2002). Inward rectifier K^+ current under physiological cytoplasmic conditions in guinea-pig cardiac ventricular cells. *J Physiol* **540**, 831–841.

Kubo Y, Baldwin TJ, Jan YN & Jan LY (1993). Primary structure and functional expression of a mouse inward rectifier potassium channel. *Nature* **362**, 127–133.

Kubo Y & Murata Y (2001). Control of rectification and permeation by two distinct sites after the second transmembrane region in Kir2.1 K^+ channel. *J Physiol* **531**, 645–660.

Kurachi Y (1985). Voltage-dependent activation of the inward-rectifier potassium channel in the ventricular cell membrane of guinea-pig heart. *J Physiol* **366**, 365–385.

Leech CA & Stanfield PR (1981). Inward rectification in frog skeletal muscle fibres and its dependence on membrane potential and external potassium. *J Physiol* **319**, 295–309.

Lopatin AN, Makhina EN & Nichols CG (1994). Potassium channel block by cytoplasmic polyamines as the mechanism of intrinsic rectification. *Nature* **372**, 366–369.

Lopatin AN, Makhina EN & Nichols CG (1995). The mechanism of inward rectification of potassium channels: 'long-pore plugging' by cytoplasmic polyamines. *J Gen Physiol* **106**, 923–955.

Lopatin AN & Nichols CG (2001). Inward rectifiers in the heart: an update on I_{K1}. *J Mol Cell Cardiol* **33**, 625–638.

Lu T, Nguyen B, Zhang X & Yang J (1999). Architecture of a K^+ channel inner pore revealed by stoichiometric covalent modification. *Neuron* **22**, 571–580.

Luo CH & Rudy Y (1994). A dynamic model of the cardiac ventricular action potential. I. Simulations of ionic currents and concentration changes. *Circ Res* **74**, 1071–1096.

Matsuda H (1988). Open-state substructure of inwardly rectifying potassium channels revealed by magnesium block in guinea-pig heart cells. *J Physiol* **397**, 237–258.

Matsuda H & Noma A (1984). Isolation of calcium current and its sensitivity to monovalent cations in dialysed ventricular cells of guinea-pig. *J Physiol* **357**, 553–573.

Matsuda H, Oishi K & Omori K (2003). Voltage-dependent gating and block by internal spermine of the murine inwardly rectifying K^+ channel, Kir2.1. *J Physiol* **548**, 361–371.

Matsuda H, Saigusa A & Irisawa H (1987). Ohmic conductance through the inwardly rectifying K channel and blocking by internal Mg^{2+}. *Nature* **325**, 156–159.

Matsuoka S, Sarai N, Kuratomi S, Ono K & Noma A (2003). Role of individual ionic current systems in ventricular cells hypothesized by a model study. *Jpn J Physiol* **53**, 105–123.

Nakamura TY, Artman M, Rudy B & Coetzee WA (1998). Inhibition of rat ventricular I_{K1} with antisense oligonucleotides targeted to Kir2.1 mRNA. *Am J Physiol* **274**, H892–H900.

Niwa H, Yamamura K & Miyazaki J (1991). Efficient selection for high-expression transfectants by a novel eukaryotic vector. *Gene* **108**, 193–200.

Oliva C, Cohen IS & Pennefather P (1990). The mechanism of rectification of i_{K1} in canine Purkinje myocytes. *J Gen Physiol* **96**, 299–318.

Picones A, Keung E & Timpe LC (2001). Unitary conductance variation in Kir2.1 and in cardiac inward rectifier potassium channels. *Biophys J* **81**, 2035–2049.

Shieh R-C, John SA, Lee J-K & Weiss JN (1996). Inward rectification of the IRK1 channel expressed in *Xenopus* oocytes: effects of intracellular pH reveal an intrinsic gating mechanism. *J Physiol* **494**, 363–376.

Shinga J, Kashiwagi K, Tashiro K, Igarashi K & Shiokawa K (1996). Maternal and zygotic expression of mRNA for S-adenosylmethionine decarboxylase and its relevance to the unique polyamine composition in *Xenopus* oocytes and embryos. *Biochim Biophys Acta* **1308**, 31–40.

Silver MR & DeCoursey TE (1990). Intrinsic gating of inward rectifier in bovine pulmonary artery cells in the presence or absence of Mg^{2+}. *J Gen Physiol* **96**, 109–133.

Stanfield PR, Davies NW, Shelton PA, Khan IA, Brammar WJ, Standen NB & Conley EC (1994*a*). The intrinsic gating of inward rectifier K^+ channels expressed from the murine IRK1 gene depends on voltage, K^+ and Mg^{2+}. *J Physiol* **475**, 1–7.

Stanfield PR, Davies NW, Shelton PA, Sutcliffe MJ, Khan IA, Brammar WJ & Conley EC (1994*b*). A single aspartate residue is involved in both intrinsic gating and blockage by Mg^{2+} of the inward rectifier, IRK1. *J Physiol* **478**, 1–6.

Stanfield PR, Nakajima S & Nakajima Y (2002). Constitutively active and G-protein coupled inward rectifier K^+ channels: Kir2.0 and Kir3.0. *Rev Physiol Biochem Pharmacol* **145**, 47–179.

Taglialatela M, Ficker E, Wible BA & Brown AM (1995). C-terminus determinants for Mg^{2+} and polyamine block of the inward rectifier K^+ channel IRK1. *EMBO J* **14**, 5532–5541.

Tourneur Y, Mitra R, Morad M & Rougier O (1987). Activation properties of the inward-rectifying potassium channel on mammalian heart cells. *J Membr Biol* **97**, 127–135.

Vandenberg CA (1987). Inward rectification of a potassium channel in cardiac ventricular cells depends on internal magnesium ions. *Proc Natl Acad Sciences U S A* **84**, 2560–2564.

Wible BA, Taglialatela M, Ficker E & Brown AM (1994). Gating of inwardly rectifying K^+ channels localized to a single negatively charged residue. *Nature* **371**, 246–249.

Woodhull AM (1973). Ionic blockage of sodium channels in nerve. *J Gen Physiol* **61**, 687–708.

Xie LH, John SA & Weiss JN (2002). Spermine block of the strong inward rectifier potassium channel Kir2.1: dual roles of surface charge screening and pore block. *J Gen Physiol* **120**, 53–66.

Yang J, Jan YN & Jan LY (1995). Control of rectification and permeation by residues in two distinct domains in an inward rectifier K^+ channel. *Neuron* **14**, 1047–1054.

Zaritsky JJ, Redell JB, Tempel BL & Schwarz TL (2001). The consequences of disrupting cardiac inwardly rectifying K^+ current (I_{K1}) as revealed by the targeted deletion of the murine *Kir2.1* and *Kir2.2* genes. *J Physiol* **533**, 697–710.

Acknowledgements

We thank Professor K. Igarashi (Chiba University, Japan) and Professor Y. Kubo (Tokyo Medical and Dental University, Japan) for invaluable discussions. This work was supported by Grants-in-Aid for Scientific Research from the Ministry of Education, Culture, Sports, Sciences, and Technology of Japan.